

Synthesis, spectral, DFT calculations and antibacterial studies of Fe(III) complexes of new fluorescent Schiff bases derived from imidazo[4',5':3,4]benzo[1,2-c]isoxazole

Shirin Ramezani | Mehdi Pordel  | Abolghasem Davoodnia

Department of Chemistry, Mashhad Branch, Islamic Azad University, Mashhad, Iran

Correspondence

Mehdi Pordel, Department of Chemistry, Mashhad Branch, Islamic Azad University, Mashhad, Iran.
Email: mehdipordel58@mshdiau.ac.ir

New fluorescent heterocyclic ligands were synthesized by the reaction of 8-(4-chlorophenyl)-3-alkyl-3*H*-imidazo[4',5':3,4]benzo [1,2-*c*]isoxazol-5-amine with *p*-hydroxybenzaldehyde and *p*-chlorobenzaldehyde in good yields. The coordination ability of the ligands with Fe³⁺ ion was examined in an aqueous metanolic solution. Schiff base ligands and their metal complexes were characterized by elemental analyses, IR, UV-vis, mass, and NMR spectra. The optical properties of the compounds were investigated and the results showed that the fluorescence of all compounds is intense and their obtained emission quantum yields are around 0.15 – 0.53. Optimized geometries and assignment of the IR bands and NMR chemical shifts of the new complexes were also computed by using density functional theory (DFT) methods. The DFT-calculated vibrational wavenumbers and NMR chemical shifts are in good agreement with the experimental values, confirming suitability of the optimized geometries for Fe(III) complexes. Also, the 3D-distribution map for HOMO and LUMO of the compounds were obtained. The new compounds showed potent antibacterial activity and their antibacterial activity (MIC) against Gram-positive and Gram-negative bacterial species were also determined. Results of antibacterial test revealed that coordination of ligands to Fe(III) leads to improvement in the antibacterial activity.

KEYWORDS

antibacterial activity, bidentate ligand, density functional theory, Fe(III) complex, Schiff base

1 | INTRODUCTION

One of the most interesting areas of coordination chemistry is the interaction of transition metal ions with biological molecules. There are many metal complexes that can use as drugs and chemotherapeutic agents.^[1]

Iron is one of the essential mineral that can function as regulators, activators, transmitters, and controllers of various enzymatic reactions.^[2,3] In hence, the iron complexes have received considerable attention owing to their effective biological importance such as antibacterial^[4,5] antifungal^[6] antiviral^[7] antiproliferative^[8] and anticancer

activity.^[9–11] The stabilities and coordination chemistry of Fe(III) with bidentate ligands^[12,13] have also resulted from their efficacy as oral iron chelating agents^[14,15] and as agents for the treatment of iron overload conditions.^[16–18]

Benzo[1,2-*c*]isoxazoles are an important class of heterocyclic pharmaceuticals and bioactive compounds which are prescribed as antipsychotic risperidone^[19] and anti-HIV drugs^[20] and play a key role in many organic reactions.^[21] Isoxazole-metal complexes are often postulated as intermediates in reactions of considerable synthetic utility, for example the reductive ring opening of isoxazoles. Several isoxazole-metal complexes have been reported

and well characterized. In a review of the literature of isoxazole-metal complexes,^[22] the binding characteristics of the isoxazoles in the complexes have been examined, and some tentative conclusions regarding the regularity of isoxazole complexation behavior have been discussed.

On the other hand, Schiff bases are an important class of organic ligands having considerable biological properties.^[23–25] Schiff bases have many advantages between ligands in the coordination chemistry. They are the most versatile studied ligands in coordination chemistry because of their structural varieties and very unique characteristics. These findings promoted us to the synthesis and characterization of two new fluorescent heterocyclic Schiff-base ligands derived from 2-8-(4-chlorophenyl)-3-alkyl-3H-imidazo[4',5':3,4]benzo [1,2-c]isoxazol-5-amine and their Fe(III) complexes. In addition, antibacterial activities of the new ligands and complexes against gram positive and negative bacterial species were studied.

2 | EXPERIMENTAL

2.1 | Equipment and materials

Melting points were measured on an Electrothermaltyp-9100 melting-point apparatus. The FT-IR (as KBr discs) spectra were obtained on a Tensor 27 spectrometer and only noteworthy absorptions are listed. The ¹³C NMR (100 MHz), ¹H NMR (400 MHz) and NOESY spectra were recorded on a Bruker Avance DRX-400 spectrometer. Chemical shifts are reported in ppm downfield from TMS as internal standard; coupling constant *J* is given in Hz. The mass spectrum was recorded on a Varian Mat, CH-7 at 70 eV and ESI mass spectrum was measured using a Waters Micromass ZQ spectrometer. Elemental analysis was performed on a Thermo Finnigan Flash EA microanalyzer. Absorption and fluorescence spectra were recorded on Varian 50-bio UV-Visible spectrophotometer and Varian Cary Eclipse spectrofluorophotometer. UV-vis and fluorescence scans were recorded from 200 to 1000 nm. Percentage of the Fe⁺³ ion was obtained by using a Hitachi 2-2000 atomic absorption spectrophotometer.

The microorganisms *Bacillus subtilis* ATCC 6633, *Pseudomonas aeruginosa* ATCC 27853 and *Escherichia coli* ATCC 25922 were purchased from Pasteur Institute of Iran and *S. aureus* methicillin resistant was isolated from different specimens which were referred to the Microbiological Laboratory of Ghaem Hospital of Medical University of Mashhad, Iran and its methicillin resistance was tested according to the NCCLS guidelines.^[26] All solvents were dried according to standard procedures. Compounds **1**,^[27] **3**,^[28] **4**^[29] and **5a,b**^[30] were obtained according to the published methods. Other reagents were commercially available.

2.2 | Computational methods

All of the calculations have been performed using the DFT method with the B3LYP functional^[31] as implemented in the Gaussian 03 program package.^[32] The 6-311+G(d,p) basis sets were employed except for the Fe atom where the LANL2DZ basis sets were used with considering its effective core potential. Geometry of the Fe complex was fully optimized, which was confirmed to have no imaginary frequency of the Hessian. Geometry optimization and frequency calculation simulate the properties in the gas/solution phases.

The fully-optimized geometries were confirmed to have no imaginary frequency of the Hessian.

The solute-solvent interactions have been investigated using one of the self-consistent reaction field methods, i.e., the sophisticated Polarizable Continuum Model (PCM).^[33]

2.3 | General procedure for the synthesis of 7a,b from 5a,b

Aldehydes **6a,b** (1 mmol) were added to a solution of compounds **5a,b** (0.34 g, 1 mmol) in EtOH (15 ml). The reaction mixture was heated under reflux for 5 hours. The solvent was removed under reduced pressure and the yellow product was filtered and washed with EtOH to give Schiff bases (**7a,b**). More purification was achieved by crystallization from suitable solvent such as acetone.

(*E*)-4-(((8-(4-chlorophenyl)-3-propyl-3H-imidazo[4',5':3,4]benzo[1,2-c]isoxazol-5-yl) imino) methyl)phenol (**7a, L1**) was obtained as a yellow powder. m.p.: 149–154 °C. ¹H NMR (CDCl₃): δ 0.91 (t, *J* = 7.5 Hz, 3H, CH₃), 1.80–1.91 (m, 2H, CH₂), 4.37 (t, *J* = 7.5 Hz, 2H, NCH₂), 6.95 (d, *J* = 9.0 Hz, 2H, Ar H), 7.69 (s, 1H, Ar H), 7.73 (d, *J* = 9.0 Hz, 2H, Ar H), 7.87 (d, *J* = 9.0 Hz, 2H, Ar H), 8.31 (s, 1H, Ar H), 8.95 (d, *J* = 9.0 Hz, 2H, Ar H), 9.08 (s, 1H, CH), 10.37 (br s, 1H, OH) ppm; ¹³C NMR (CDCl₃): δ 16.1, 28.7, 51.4, 114.3, 114.7, 121.0, 131.5, 132.8, 133.7, 134.5, 135.1, 135.3, 136.1, 140.0, 140.6, 146.5, 159.9, 165.9, 166.1, 166.9 ppm. IR (KBr): 3348 cm⁻¹ (OH), 1645 cm⁻¹ (CH=N). MS (m/z) 432 (M⁺+2). Anal. Calcd for C₂₄H₁₉ClN₄O₂ (430.9): C, 66.90; H, 4.44; N, 13.00. Found: C, 66.78; H, 4.41; N, 12.82.

(*E*)-3-Butyl-*N*-(4-chlorobenzylidene)-8-(4-chlorophenyl)-3H-imidazo[4',5':3,4]benzo[1,2-c] isoxazol-5-amine (**7b, L2**) was obtained as a yellow powder. m.p: 181–184 °C; yield: 75%. ¹H NMR (CDCl₃): δ 0.92 (t, *J* = 7.5 Hz, 3H, CH₃), 1.24–1.37 (m, 2H, CH₂), 1.75–1.82 (m, 2H, CH₂), 4.31 (t, *J* = 7.5 Hz, 2H, NCH₂), 7.62 (d, *J* = 9.0 Hz, 2H, Ar H), 7.69 (d, *J* = 9.0 Hz, 2H, Ar H), 7.75 (s, 1H, Ar H), 7.98 (d, *J* = 9.0 Hz, 2H, Ar H), 8.30 (s, 1H, Ar H), 8.88 (d, *J* = 9.0 Hz, 2H, Ar H), 9.25 (s, 1H, CH=N) ppm; ¹³C NMR (CDCl₃): δ 13.9, 19.8, 32.6, 44.9, 109.4, 112.6,

126.6, 129.0, 129.5, 129.7, 130.0, 130.6, 131.5, 131.7, 134.1, 135.4, 135.6, 136.6, 142.1, 154.7, 161.2, 161.2 ppm. IR (KBr): 1643 cm^{-1} (CH=N). MS (m/z) 466 ($M^+ + 4$). Anal. Calcd for $\text{C}_{25}\text{H}_{20}\text{Cl}_2\text{N}_4\text{O}$ (463.4): C, 64.80; H, 4.35; N, 12.09. Found: C, 64.31; H, 4.32; N, 12.01.

2.4 | General procedure for the synthesis of complexes **8a,b** from ligands **7a,b**

To the yellow solution of ligand **7a,b** (467 mmol) in aqueous methanolic solution (20 ml, MeOH, H_2O , 10:90) iron (III) chloride (0.476, 294 mmol) was added, resulting in color change to deep green. The reaction was carried out for another 6 h in room temperature. The complex was isolated by evaporation of the solvent and washed with cold MeOH and then H_2O .

[Fe(L1)₂]Cl₃·2(H₂O) (**8a**): was obtained as a dark green powder. mp > 300 °C (decomp). ¹H NMR (DMSO-*d*₆): δ 0.93 (t, $J = 7.5$ Hz, 6H, CH₃), 1.78–1.89 (m, 4H, CH₂), 4.31 (t, $J = 7.5$ Hz, 4H, NCH₂), 7.01 (d, $J = 9.0$ Hz, 4H, Ar H), 7.65–7.85 (m, 10H, Ar H), 8.33 (s, 2H, Ar H), 8.98 (d, $J = 9.0$ Hz, 4H, Ar H), 9.16 (s, 2H, CH), 10.75 (br s, 2H, OH). IR (KBr): 3382 cm^{-1} (OH), ESI-MS (+) m/z (%): 917 [Fe(L2)₂]³⁺. Anal. Calcd for $\text{C}_{48}\text{H}_{42}\text{Cl}_5\text{FeN}_8\text{O}_6$ (1060.0): C, 54.39; H, 3.99; N, 10.57; Fe, 5.27. Found: C, 54.01; H, 3.93; N, 11.04; Fe, 4.68.

[Fe(L2)₂]Cl₃·2(H₂O) (**8b**): was obtained as a dark green powder. mp > 300 °C (decomp). ¹H NMR (DMSO-*d*₆): δ 0.85 (t, $J = 7.0$ Hz, 6H, CH₃), 1.20–1.23 (m, 4H, CH₂), 1.69–1.72 (m, 4H, CH₂), 4.25 (t, $J = 7.0$ Hz, 4H, NCH₂), 7.66 (d, $J = 9.0$ Hz, 4H, Ar H), 7.71 (s, 2H, Ar H), 7.74 (d, $J = 9.0$ Hz, 4H, Ar H), 7.95 (d, $J = 9.0$ Hz, 4H, Ar H), 8.33 (s, 2H, Ar H), 8.89 (d, $J = 9.0$ Hz, 4H, Ar H), 9.12 (s, 2H, CH=N) ppm; IR (KBr): 3435, cm^{-1} (OH), ESI-MS (+) m/z (%): 982 [Fe(L1)₂]³⁺. Anal. Calcd for $\text{C}_{50}\text{H}_{44}\text{Cl}_7\text{FeN}_8\text{O}_4$ (1110.9): C, 53.38; H, 3.94; N, 9.96; Fe, 4.96. Found: C, 52.90; H, 3.89; N, 10.36; Fe, 4.46.

3 | RESULTS AND DISCUSSION

3.1 | Synthesis and structure of the new ligands **7a,b** and complexes **8a,b**

In order to the synthesis of new heterocyclic Schiff-base ligands, the commercially available 5-nitro-1*H*-benzimidazole was alkylated with 1-bromopropane and 1-bromobutane in KOH and DMF to give 1-alkyl-5-nitro-1*H*-benzimidazole (**1a,b**).^[27] 3-Alkyl-8-(4-chlorophenyl)-3*H*-imidazo [4',5':3,4]benzo[1,2-*c*]isoxazoles (**3a,b**) were prepared from the reaction of 1-alkyl-5-nitro-1*H*-benzimidazole **1a,b** with (4-chlorophenyl)acetonitrile (**2**) in basic MeOH solution.^[28] Regioselective nitration of **3a,b** using a mixture of sulfuric acid and potassium nitrate

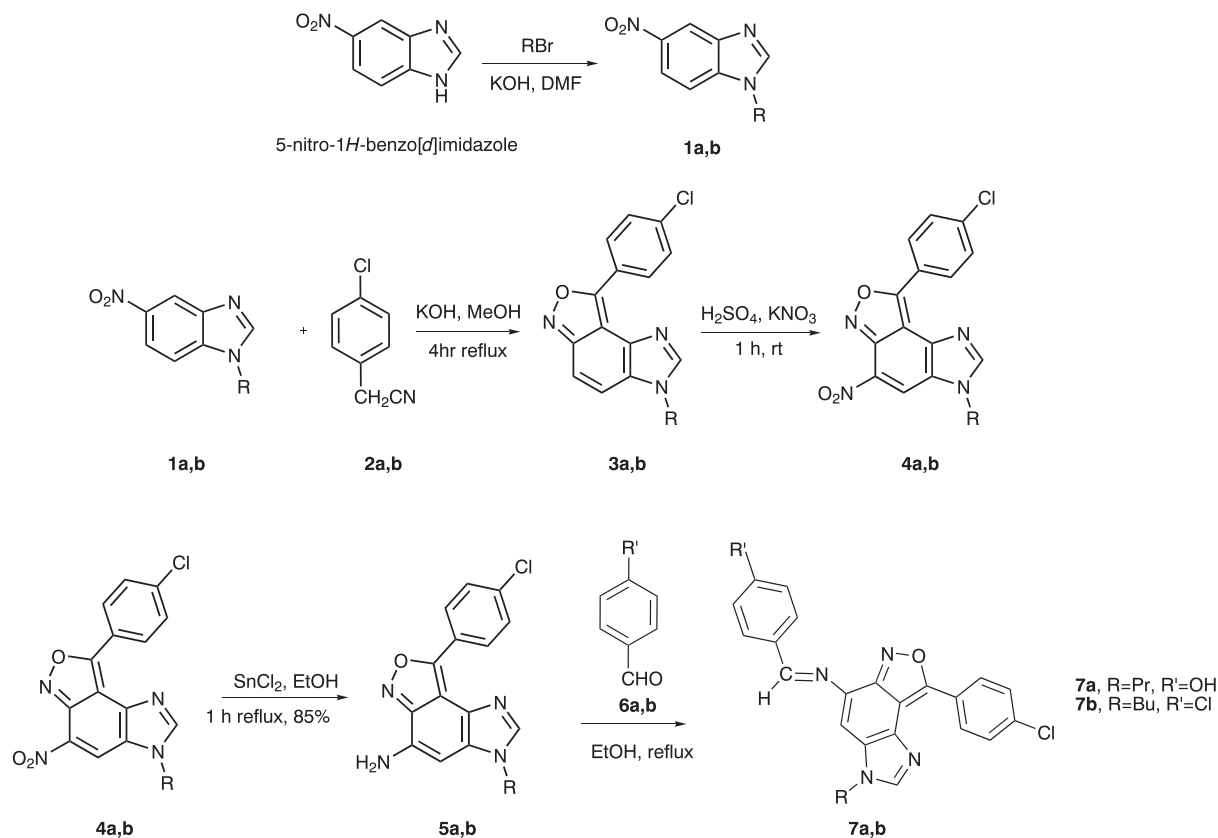
led to the formation of 3-alkyl-8-(4-chlorophenyl)-5-nitro-3*H*-imidazo[4',5':3,4]benzo[1,2-*c*]isoxazoles **4a,b** in good yield.^[29] Reduction of compounds **4a,b** in EtOH by SnCl₂, gave the 8-(4-chlorophenyl)-3-alkyl-3*H*-imidazo [4',5':3,4]benzo[1,2-*c*]isoxazol-5-amines (**5a,b**) in high yields. Finally, new heterocyclic Schiff-bases **7a,b** were obtained by the reaction of amines **5a,b** with aldehydes **6a,b** in good yields (Scheme 1).

The structural assignments of compounds **7a,b** were determined based on the analytical and spectral data. For example, in the ¹H NMR spectrum of compound **7a** there is an exchangeable peak at δ 10.37 ppm assignable to OH group proton. Also, there are four doublet signals ($\delta = 6.95, 7.73, 7.78, 8.95$ ppm) and two singlet signals ($\delta = 7.69$ and 8.31 ppm) attributed to ten protons of aromatic rings. Also, there is a singlet signal ($\delta = 9.08$) assignable to the imine CH proton. In addition, 20 different carbon atom signals are observed in the ¹³C NMR spectrum of compound **7a**. Moreover, the IR spectrum of compound **7a** in KBr revealed a broad absorption band at 3348 cm^{-1} assignable to OH group. All this evidence taken in conjunction with molecular ion peak at m/z 432 [$M+2$]⁺ support the structure of Schiff-base **7a**. In addition, the data from NOESY experiment showed a cross-peak between the H-4 proton (δ_{H} 7.69, s, CH-benzene) and the imine CH proton (δ_{H} 9.08), confirming the *E* configuration of the product structure (Scheme 2). Furthermore, as can be seen in Scheme S1 (Supplementary Data), there are a massive cross-peak between the H-4 proton and the N-3 alkyl group (δ_{H} 4.37 (t, $J = 7.2$ Hz, NCH₂) and interactions between proton of imidazole ring (δ_{H} 8.31, s, CH-imidazole) and CH₂ protons of propyl group (δ_{H} 4.37 (t, $J = 7.2$ Hz, NCH₂).

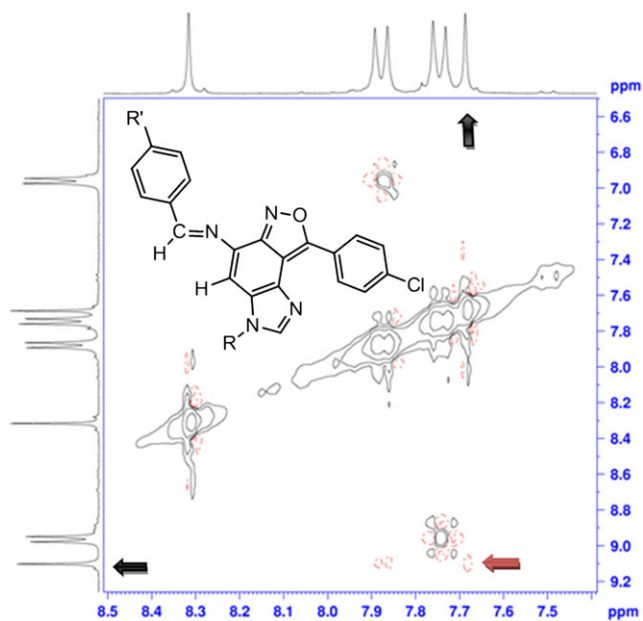
The coordination ability of Schiff-bases **7a,b** with Fe³⁺ ion was examined in an aqueous methanolic solution. The elemental analysis results (Experimental section) and the stoichiometry of the deep green complexes obtained by Job's method (Figures S1 and S2, Supplementary Data),^[34] proposed the [Fe(L)₂]Cl₃·2(H₂O) formulae for the complexes (Scheme 3). Electrospray ionisation mass spectrometry (ESI-MS) of the complexes **8a,b** showed molecular ion peak at m/z 917 ([Fe(L1)₂]³⁺) and m/z 982 ([Fe(L2)₂]³⁺) which strongly confirmed that molar ratio between Fe (III) ions and ligands in the complexes is 1:2. Moreover, basic molecular ion peak at m/z 159 (C₈H₅N₃O) can be related to imidazo[4',5':3,4]benzo[1,2-*c*]isoxazole scaffold in ligands and complexes.

3.2 | Photophysical properties of the new ligands and complexes

Compounds **7a,b**, and Iron complexes **8a,b** were spectrally characterized by UV-Vis and fluorescence spectroscopy in the wavelength range of 200–1000 nm.



SCHEME 1 Synthesis of the new ligands **7a,b**



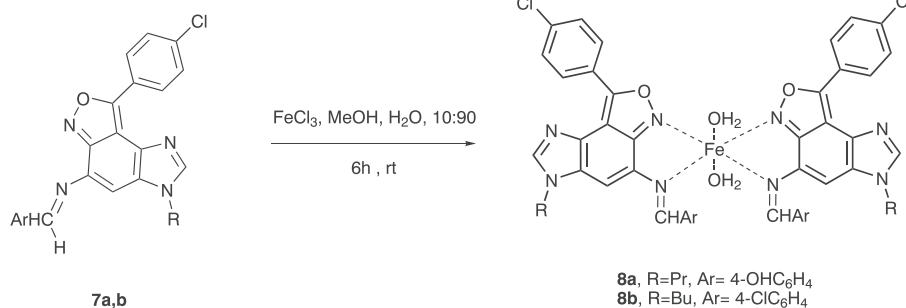
SCHEME 2 NOESY spectrum of compound **7a**

The absorption and fluorescence emission spectra of the ligands **7a,b** and iron (III) complexes **8a,b** are shown in Figures 1 and 2, respectively. Also, numerical spectral data are presented in Table 1. Values of extinction

coefficient (ϵ) were calculated as the slope of the plot of absorbance vs concentration. As depicted in Figure 1, the spectra of complexes have an absorption maximum at 750 nm at which the ligand has no absorbance. An efficient charge transfer of electron from p-orbital on ligand to Fe (III) d-orbital can be considered as the main reason for the color of the complexes described as Ligand to-Metal charge transfer (LMCT).^[35] Also, Schiff-base ligands **7a,b**, and Iron complexes **8a,b** produced fluorescence at concentration 1×10^{-5} M in MeOH (Figure 2). The fluorescence quantum yield of the compounds was determined *via* comparison methods, using fluorescein as a standard sample in 0.1 M NaOH and MeOH solution.^[36] The used value of the fluorescein emission quantum yield is 0.79 and the obtained emission quantum yields of the new compounds are around 0.15 – 0.53. As can be seen from Table 1, extinction coefficient (ϵ) in Schiff-base **7b**, fluorescence intensity and the emission quantum yield in Schiff-base **7a** were the biggest values.

3.3 | DFT calculations

According to our experimental results and reported literatures,^[37] an octahedral geometry was proposed for the



SCHEME 3 Synthesis of Fe(III) complexes **8a,b**

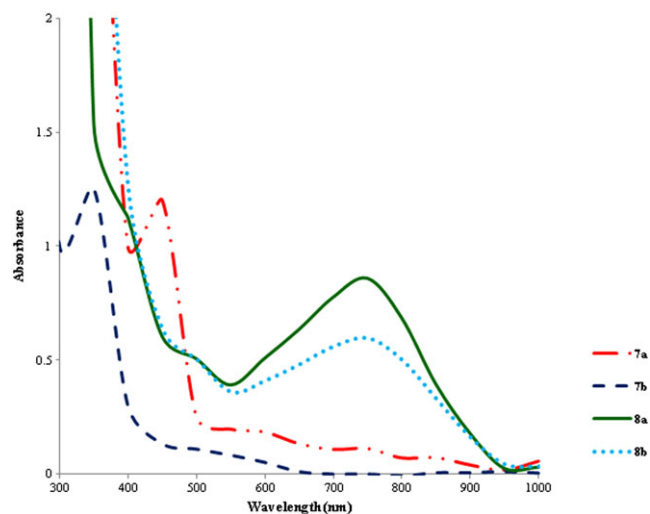


FIGURE 1 The absorption spectra of the ligands **7a,b** and Fe(III) complexes **8a,b** in MeOH solution (2×10^{-4} M)

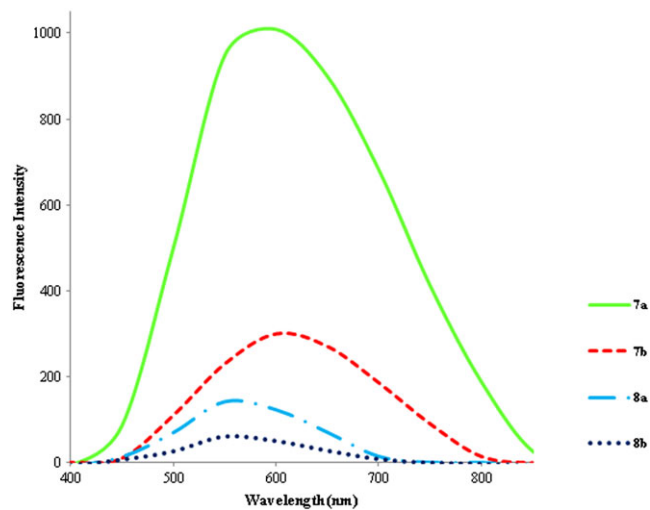


FIGURE 2 The fluorescence emission spectra of the ligands **7a,b** and Fe(III) complexes **8a,b** in MeOH solution (1×10^{-5} M)

iron complexes **8a,b**. We performed DFT calculations at the B3LYP/6-311+G(d,p) level to gain a deeper insight into the geometries and role of HOMO and LUMO

TABLE 1 Spectroscopic data for the new compounds **7a,b** and **8a,b** at 298 K

Dye	7a	7b	8a	8b
λ_{abs} (nm) ^a	440	360	750	750
$\epsilon \times 10^{-3}$ [(mol L ⁻¹) ⁻¹ cm ⁻¹] ^b	6.00	6.25	4.30	3.00
λ_{flu} (nm) ^c	600	595	550	550
Φ_F ^d	0.53	0.32	0.24	0.15

^aWavelengths of maximum absorbance (λ_{abs}).

^bExtinction coefficient.

^cWavelengths of fluorescence emission (λ_{flu}) with excitation at 400 nm.

^dFluorescence quantum yield.

frontier orbitals in the UV-visible absorption spectra of Schiff-bases **7a,b** and iron complexes **8a,b**. Geometry of the complex **8b** was optimized in both of the gas phase and the PCM model, where the methanol was the used solvent. The optimized geometry of the ligands **7a,b** can be found in Figure 3. The optimized geometry of the complex **8b** with labeling of its atoms is also depicted in Figure 4. Some of the calculated structural parameters of the Fe(III) complex are collected in Table 2.

In the optimized geometry of the complex **8b**, the ligand **7b** acts as a bidentate ligand, coordinates to the Fe(III) *via* nitrogen atom of the imine group ($-N=CH$) and nitrogen atom of the isoxazole ring.

Except of the butyl group, the ligands **7b** are planar. The aromatic rings of the ligand are in a same plane. Also, both of the ligands are in a same plane forming a square plane of the octahedral complex. Two other positions of the complex are filled by two H₂O molecules, which are *Trans* to each other. The H₂O ligands are perpendicular to the square plane of the complex. The Fe-O and Fe-N Lengths bonds are listed in Table 2.

3.3.1 | NMR spectra

The DFT computed ¹H NMR chemical shifts (δ) of Fe(III) complex **8b** are listed in Table 3 together with the

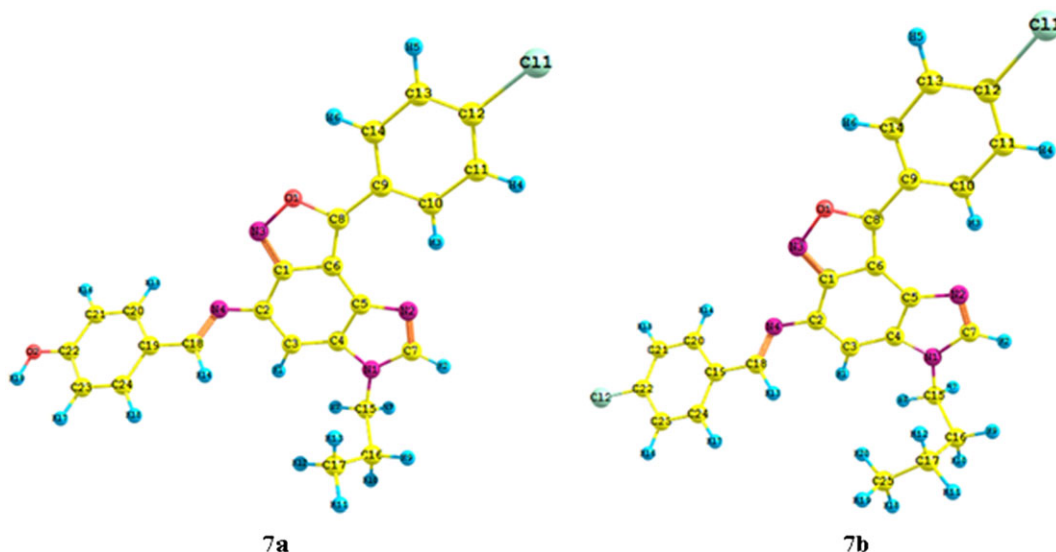


FIGURE 3 The optimized geometry of the ligands **7a,b**

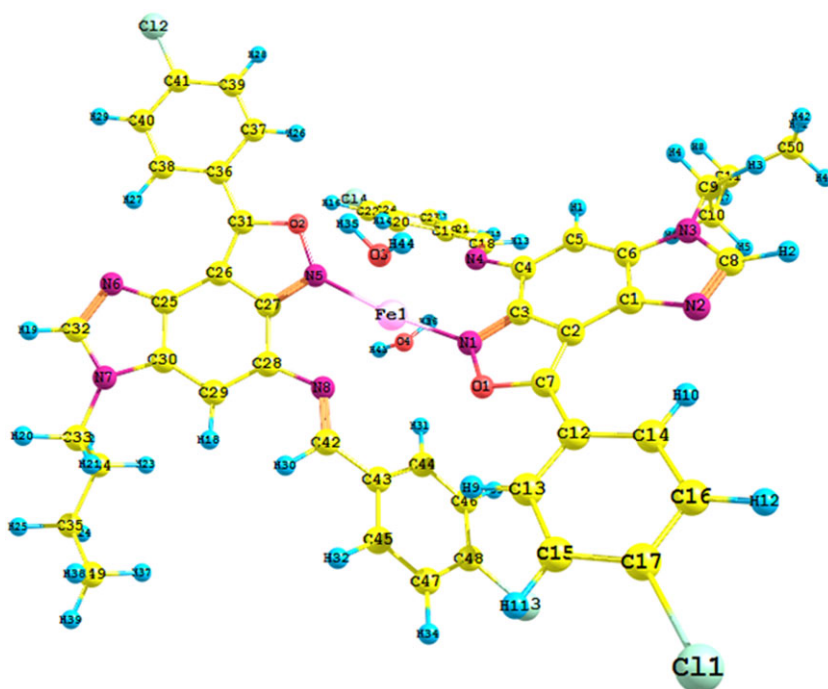


FIGURE 4 The optimized geometry of the iron(III) complex **8b**

experimental values for comparison. The atoms are numbered as in Figure 4.

As seen in Table 3, the DFT-calculated NMR chemical shifts are in good agreement with the experimental values, confirming suitability of the optimized geometries for Fe(III) complex **8b**.

3.3.2 | Vibrational spectroscopy

The vibrational modes of Fe complex **8b** were also analyzed by comparing the experimental and DFT-computed IR spectra. Assignment of the selected-vibrational

frequencies is gathered in Table 4. There is good agreement between the experimental and DFT-calculated frequencies of the high spin complex, confirming validity of the optimized geometry as a proper structure for the complex **8b**.

The 3D-distribution map for the highest-occupied-molecular orbital (HOMO) and the lowest-unoccupied-molecular orbital (LUMO) of the ligands **7a,b** and the complex **8b** are shown in Figure 5. As seen, the HOMO orbital of the ligands is localized on the benzimidazole and isoxazole rings. But the LUMO orbital is mainly localized on the benzene ring and its substitutions. Since, in

TABLE 2 Selected structural parameters of Fe(III) complex **8b**

Bond	Bond length (Å ^b)	Angle	(°)	Dihedral angle	(°)
Fe-N1	2.076	N1-Fe-N5	163.54	N1-N5-N4-N8	27.598
Fe-N4	2.729	N1-Fe-N4	70.055	N1-N5-N4-Fe	12.668
Fe-N5	2.124	N5-Fe-N8	75.787	O2-N5-Fe-O3	70.171
Fe-N8	2.364	N1-Fe-N8	107.593	O2-N5-Fe-O4	-95.595
Fe-O3	2.203	N4-Fe-N5	112.01	O2-N5-Fe-N8	177.499
Fe-O4	2.152	N1-Fe-O4	100.325	C27-N5-Fe-O4	93.484
N5-O2	1.398	N5-Fe-O3	78.28	C27-N5-Fe-O3	-100.750
O2-C31	1.360	N1-Fe-O3	85.27	C27-C28-N8-O4	-40.017
C31-C26	1.401	N5-Fe-O4	95.834	C28-N8-Fe-N5	-6.741
C26-C27	1.425	O3-Fe-O4	164.76	C28-N8-N1-Fe	-34.899
C27-C28	1.430	Fe-N5-C27	116.093	O1-C7-C2-C3	-0.256
C31-C36	1.446	N5-C27-C28	123.00	O1-C7-C12-C13	-0.327
C36-C38	1.410	C3-N1-Fe	123.09	C7-C2-C1-N2	0.894
C28-N8	1.415	Fe-O1-N1	120.3	C6-C1-N2-C8	-0.030
N8-C42	1.305	C3-N1-O1	123.09	N2-C8-N3-C6	-0.683
C27-N5	1.333	Fe-O3-N1	45.533	C2-C7-C12-C14	-0.683
C25-N6	1.363	C3-N1-O1	105.52	N5-C27-C26-C31	-0.695
N6-C32	1.323	N1-O1-C7	110.66	C1-C6-N3-C8	0.600
C32-N7	1.364	C1-C6-N3	104.81	C3-C4-C5-C6	2.178
N7-C33	1.469	C1-N2-C8	104.656	N3-C9-C10-C11	178.514

TABLE 3 DFT calculated and experimental ¹H NMR chemical shifts of Fe(III) complex **8b** in DMSO solution, δ [ppm]

Atomic number	Chemical shift		Atomic number	Chemical shift	
	Cal.	Exp.		Cal.	Exp.
H30	9.28	9.12	H31	7.49	7.66
H12	9.06	8.89	H20	4.10	4.24
H19	8.18	8.33	H22	1.75	1.69–1.71
H28	7.80	7.95	H24	1.32	1.20–1.23
H10	7.77	7.74	H36	0.97	0.85
H18	7.54	7.71			

the ligands **7a,b**, electron transition from the HOMO orbital to the LUMO orbital is $\pi \rightarrow \pi^*$ transition. On the other hand, the HOMO and LUMO frontier orbitals of the complex **8b** species are mainly localized on the isoxazole ring and Fe atom, respectively. It implies that electron transition from the HOMO orbital to the LUMO orbital is Ligand to-Metal charge transfer (LMCT).^[35]

The energy difference between the HOMO and LUMO frontier orbitals is one of the important characteristics of molecules, which has a determining role in such cases as electric properties, electronic spectra and photochemical reactions. Energy separation between the HOMO

and LUMO ($\Delta\epsilon = \epsilon_{\text{LUMO}} - \epsilon_{\text{HOMO}}$) of **7a**, **7b** and **8b** is 3.22 eV (385 nm), 3.29 eV (377 nm) and 1.75 eV (708 nm), compared with the experimental values of 440, 360 and 750 nm, respectively.

3.4 | Antibacterial studies

The antibacterial activity of the ligands **7a,b** and complexes **8a,b** was tested against a panel of strains of Gram negative bacterial (*Pseudomonas aeruginosa* (ATCC 27853) and *Escherichia coli*, (ATCC 25922)) and Gram positive (*Staphylococcus aureus* methicillin resistant *S. aureus*

TABLE 4 Selected experimental and calculated IR vibrational frequencies (cm^{-1}) of Fe(III) complex **8b**

Experimental frequency	Calculated frequency	Intensity ($\text{km}\cdot\text{mol}^{-1}$)	Vibrational assignment
504 (w)	513	64	$\nu_{\text{sym}}(\text{Fe-N})$
549 (w)	562	186	$\nu_{\text{asym}}(\text{Fe-N})$
834(s)	833	97	ν_{sym} (C-cl) of the benzene rings involving the -cl substituent
958(w)	905	163	δ_{wagging} of the $-\text{CH}_2$ moieties
	931	1135	Breathing of the aromatic rings
1016 (m)	970, 972	183, 206	$\nu(\text{N1-O1}, \text{N4-O2}) + \nu(\text{C-C})$ aliphatic
	1014	108	$\nu(\text{C4-N7}, \text{C18-N8})$
1045 (s)	1043	935	$\nu(\text{C29-N3}, \text{C33-N6}) + \nu(\text{C-cl}) + \nu(\text{C-O})$
	1054, 1062	1085, 1273	$\nu(\text{C-cl}) + \nu_{\text{asym}}(\text{C2-O1-N1}, \text{C16-O2-N4})$
1091 (s)	1082	145	$\nu_{\text{sym}}(\text{C-C})$ aliphatic
	1107	33	δ_{ip} (aromatic hydrogens)
1187 (m, sh)	2007	420	$\nu(\text{C4-N7}, \text{C18-N8}, \text{C2-O1}, \text{C16-O2})$
	1113	652	$\nu(\text{C2-C9}, \text{C16-C23})$
1211 (m)	1214	203	$\nu(\text{C2-O1}, \text{C16-O2})$
1263(m)	1235	658	$\nu(\text{C29-N3}, \text{C33-N6})$
	1274	118	$\nu_{\text{asym}}(\text{C7-N2-C8}, \text{C21-N5-C22})$
1318 (m)	1323	2745	$\nu(\text{C29-N3}, \text{C33-N6})$
1375 (s)	1402	1531	$\nu(\text{C=C}, \text{C=N})$ of the aromatic rings
1449 (vs)	1404	833	$\nu(\text{C=C}, \text{C=N})$ of the aromatic rings
	1433	86	$\delta_{\text{oscissoring}}$ of the methyl groups
	1452	175	$\delta_{\text{oscissoring}}$ of the $-\text{CH}_2$ moieties
1492 (vs, sh)	1475	83	$\nu_{\text{asym}}(\text{C-C})$ of the benzene rings involving the -cl substituent
	1489	68	
1564(vs)	1532	1989	$\nu(\text{C=C}, \text{C=N})$ of the aromatic rings
	1555	3995	
	1574	1087	
1630(m)	1627	49	$\nu_{\text{asym}}(\text{C=N})$ of the imine
2870 (w)	2898, 2982	62,13	$\nu_{\text{sym}}(\text{C-H})$ of the $-\text{CH}_2$ moieties
2902(m)	2887	57	$\nu_{\text{sym}}(\text{C-H})$ of the methyl groups
2917(m)	2883-2952	7-47	$\nu_{\text{asym}}(\text{C-H})$ of the $-\text{CH}_2$ moieties
2962 (w)	2958 -2997	13-38	$\nu(\text{C-H})$ aromatic
	3024	79	$\nu(\text{C8-H2}, \text{C22-H8})$
3435 (m,br)	3381	127	$\nu_{\text{sym}}(\text{O-H})$ of the H_2O ligands
	3432	9	$\nu_{\text{asym}}(\text{O-H})$ of the H_2O ligands

Abbreviation: op, out-of-plane; ip, in-plane; w, weak; m, medium; s, strong; vs, very strong; br, broad; sh, shoulder.

(MRSA) clinical isolated and *Bacillus subtilis* (ATCC 6633)) species (Table 5) using broth microdilution method as previously described.^[38] Comparison with Ampicillin as a standard was done. The lowest concentration of the antibacterial agent that prevents growth of the test organism, as detected by lack of visual turbidity (matching the negative growth control), is designated the minimum inhibitory concentration (MIC). Experimental details of the tests can be found in our earlier study.^[39,40]

As seen in Table 5, compounds **7a,b** inhibit the metabolic growth of the tested Gram positive and negative bacteria to the same extent, but the inhibitions percent

are less than those of Ampicillin. Coordination of ligands **7a,b** to Fe(III) leads to improvement in the antibacterial activity. This can be explained by Tweedy's chelation theory,^[41] which explicated that the lipophilicity of the uncoordinated ligand can be changed by reducing of the polarizability of the M^{n+} ion via the L→M donation, and the possible electron delocalization over the metal complexes. Also, the results revealed that the complex **8a** with R= Pr and Ar= 4-OHC₆H₄ groups, displayed greater antibacterial activity against Gram-negative bacteria than did the well-known antibacterial agent Ampicillin (Table 5).

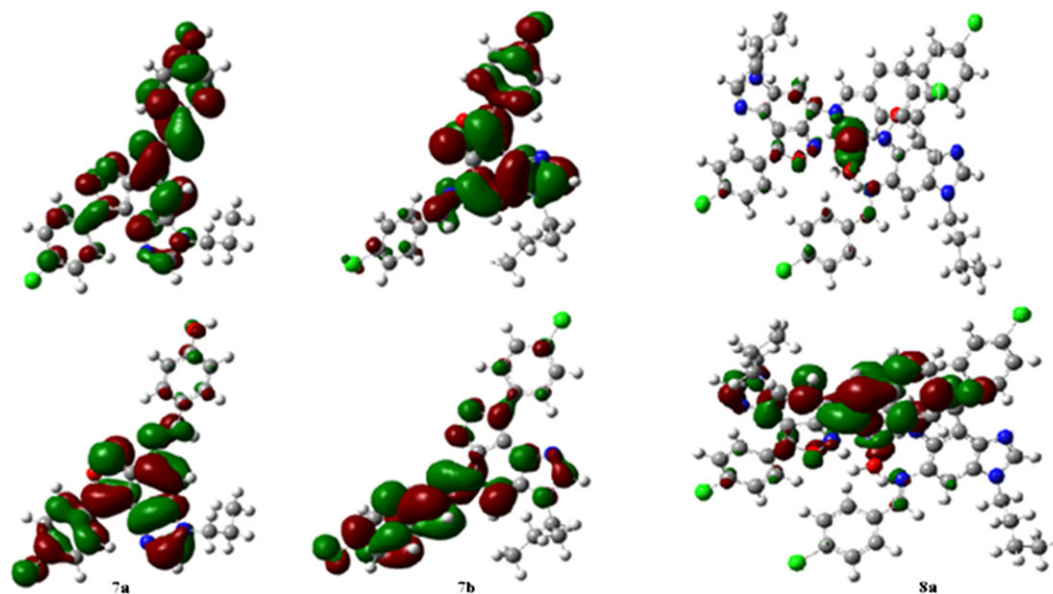


FIGURE 5 The HOMO (down) and LUMO (up) frontier orbitals of the ligands **7a,b** and complex **8b**

TABLE 5 Antibacterial activity (MIC, $\mu\text{g mL}^{-1}$) of reference and compounds **7a,b** and **8a,b**

Comps.	S.a. (MRSA)	B.s. (ATCC 6633)	P.a. (ATCC 27853)	E.c. (ATCC 25922)
7a	90	85	85	80
7b	100	100	95	95
8a	25	15	20	5
8b	40	35	35	15
Ampicillin	62	0.50	125	8

4 | CONCLUSION

In summary, we have synthesized two new fluorescent heterocyclic Schiff base ligands from the reaction of 8-(4-chlorophenyl)-3-alkyl-3*H*-imidazo[4',5':3,4]benzo [1,2-*c*]isoxazol-5-amine with *p*-hydroxybenzaldehyde and *p*-chlorobenzaldehyde. Results from NOESY experiment of the ligands confirmed the *E* configuration of Schiff-bases. Coordination of the ligands with Fe(III) cation led to the formation of deep green complexes in high yields. The structures of the complexes have been confirmed by spectral, analytical data and Job's method. Schiff-base ligands and iron complexes were spectrally characterized by UV-Vis and fluorescence spectroscopy. Studies of optical properties showed that the intensity of fluorescence emission of all compounds is high and their obtained emission quantum yields are around 0.15 – 0.53. Optimized geometries and assignment of the IR bands and NMR chemical shifts of the new complexes were also computed by DFT methods. The results revealed that the DFT-calculated

spectral properties are in good agreement with the experimental values, confirming suitability of the optimized geometries for Fe(III) complexes. Moreover, results from the antimicrobial screening tests show that new compounds are effective against standard strains of Gram-negative growth inhibitors. An improvement in the antibacterial activity is observed upon the coordination to the Fe(III) ion.

Such ligands would appear to offer a suitable template for the speciation of iron in different samples and further studies are under way to this end in our laboratory.

ACKNOWLEDGMENT

We would like to express our sincere gratitude to Research Office, Mashhad Branch, Islamic Azad University, Mashhad-Iran, for financial support of this work. We must also acknowledge Maryam Jajarmi (Khorasan Razavi Rural Water and Wastewater Co.) for her assistance in antibacterial studies.

ORCID

Mehdi Pordel  <http://orcid.org/0000-0003-3445-8792>

REFERENCES

- [1] C. J. Dhanaraj, J. Johnson, *Appl. Organomet. Chem.* **2016**, *30*, 860.
- [2] S. H. Bae, M. S. Seo, Y. M. Lee, K. B. Cho, W. S. Kim, W. Nam, *Angew. Chem. Int. Ed.* **2016**, *55*, 8027.
- [3] (a) L. C. M. Castro, H. Li, J. -B. Sortais, C. Darcel, *Green Chem.* **2015**, *17*, 2283. (b) K. Natte, W. Li, S. Zhou, H. Neumann, X.-F. W. Tetrahedron, *Lett.* **2015**, *56*, 1118. (c) B. M. Peterson, M. E. Herried, R. L. Neve, R. W. McGaff, *Dalton Trans.* **2014**, *48*, 17899.
- [4] U. Onyenze, I. E. Otuokere, J. C. Igwe, *Research J. Science and Tech.* **2016**, *8*, 215.
- [5] D. Mandal, S. Raha, T. Rakshit, A. De Das, K. C. Ghosh, P. Mitra, *J. Environ. Sociobiol.* **2016**, *1*, 15.
- [6] A. K. Hijazi, Z. A. Taha, A. M. Ajlouni, W. M. Al-Momani, T. S. Ababneh, H. M. Alshare, F. E. Kuehn, *Applied Org. metallic Chem.* **2017**, *5*, 31.
- [7] A. N. Alaghaz, M. E. Zayed, S. A. Alharbi, *J. Mol. Struct.* **2015**, *1084*, 36.
- [8] T. Fukushima, E. Taniguchi, H. Yamada, K. Kato, A. Shimizu, Y. Nishiguchi, M. Onozato, H. Ichiba, Y. Azuma, *BioMetals* **2015**, *28*, 669.
- [9] Y. Gou, J. Wang, S. Chen, Z. Zhang, Y. Zhang, W. Zhang, F. Yang, *Eur. J. Med. Chem.* **2016**, *123*, 354.
- [10] K. Saleem, W. A. Wani, A. Haque, M. N. Lone, M. F. Hsieh, M. A. Jairajpuri, I. Ali, *Future med. chem.* **2013**, *5*, 135.
- [11] D. Murtinho, Z. N. Rocha, A. S. Pires, R. P. Jiménez, A. M. Abrantes, M. Laranjo, A. C. Mamede, J. E. Casalta-Lopes, M. F. Botelho, A. A. Pais, S. C. Nunes, *Appl. Org. metal. Chem.* **2015**, *29*, 425.
- [12] M. Sova, R. Frlan, S. Gobec, G. Stavber, Z. Časar, *Appl. Organomet. Chem.* **2015**, *29*, 528.
- [13] M. Y. Khan, J. Zhou, X. Chen, A. Khan, H. Mudassir, Z. Xue, S. W. Lee, S. K. Noh, *Polymer* **2016**, *90*, 309.
- [14] M. Chieppa, V. Galleggiante, G. Serino, M. Massaro, A. Santino, *Curr. Pharm. Des.* **2017**, *23*, 2289.
- [15] M. Kono, K. Saigo, S. Yamamoto, K. Shirai, S. Iwamoto, T. Uematsu, T. Takahashi, S. Imoto, M. Hashimoto, Y. Minami, A. Wada, *Clin. Exp. Pharmacol. Physiol.* **2016**, *43*, 915.
- [16] S. M. El Sayed, A. Abou-Taleb, H. S. Mahmoud, H. Baghdadi, R. A. Maria, N. S. Ahmed, M. M. Nabo, *Med. hypotheses* **2014**, *83*, 238.
- [17] R. F. Júnior, V. B. Marques, D. O. Nunes, I. Stefanon, L. dos Santos, *Toxicol. Lett.* **2017**, *279*, 43.
- [18] G. Y. Oudit, P. H. Backx, *Can. J. Cardiol.* **2016**, *32*, 938.
- [19] M. A. Barmade, P. R. Murumkar, M. Kumar Sharma, M. Ram Yadav, *Curr. Top. Med. Chem.* **2016**, *16*, 2863.
- [20] M. Madni, S. Hameed, M. N. Ahmed, M. N. Tahir, N. A. Al-Masoudi, C. Pannecouque, *Med. Chem. Res.* **2017**, *26*, 2653.
- [21] M. A. Kalwat, Z. Huang, C. Wichaidit, K. McGlynn, S. Earnest, C. Savoia, E. M. Dioum, J. W. Schneider, M. R. Hutchison, M. H. Cobb, *ACS Chem. Biol.* **2016**, *11*, 1128.
- [22] M. S. Munsey, N. R. Natale, *Coord. Chem. Rev.* **1991**, *109*, 251.
- [23] Ö. Güngör, P. Gürkan, *J. Mol. Struct.* **2014**, *1074*, 62.
- [24] J. A. Makawana, J. Sun, H. -L. Zhu, *Bioorg. Med. Chem. Lett.* **2013**, *23*, 6264.
- [25] E. L. de Araújo, H. F. Barbosa, E. R. Dockal, É. T. Cavalheiro, *Int. J. Biol. Macromolec.* **2017**, *95*, 168.
- [26] D. Sweeney, A. Stoneburner, D. L. Shinabarger, F. F. Arhin, A. Belley, G. Moeck, C. M. Pillar, *J. Antimicrob. Chemother.* **2016**, *72*, 622.
- [27] P. N. Preston, *In The Chemistry of Heterocyclic Compounds, Part 1*, 40, John Wiley & Sons 87.
- [28] M. Rahimizadeh, M. Pordel, M. Bakavoli, Z. Bakhtiarpoor, A. Orafaie, *Monatsh. Chem.* **2009**, *140*, 633.
- [29] (a) S. Ramezani, M. Pordel, S. Beyramabadi, *J. Fluoresc.* **2016**, *26*, 513. (b) M. Rezazadeh, M. Pordel, A. Davoodnia, S. Saberi, *Chem. Hetero. Comp.* **2015**, *51*, 918.
- [30] Z. Agheli, M. Pordel, S. A. Beyramabadi, *J. Mol. Struct.* **2017**, *1130*, 55.
- [31] C. Lee, W. Yang, R. G. Parr, *Phys. Rev. B.* **1988**, *37*, 785.
- [32] M. J. Frisch, G. W. Trucks, H. B. Schlegel, G. E. Scuseria, M. A. Robb, J. R. Cheeseman, J. A. Montgomery Jr., T. Vreven, K. N. Kudin, J. C. Burant, J. M. Millam, S. S. Iyengar, J. Tomasi, V. Barone, B. Mennucci, M. Cossi, G. Scalmani, N. Rega, G. A. Petersson, H. Nakatsuji, M. Hada, M. Ehara, K. Toyota, R. Fukuda, J. Hasegawa, M. Ishida, T. Nakajima, Y. Honda, O. Kitao, H. Nakai, M. Klene, X. Li, J. E. Knox, H. P. Hratchian, J. B. Cross, V. Bakken, C. Adamo, J. Jaramillo, R. Gomperts, R. E. Stratmann, O. Yazyev, A. J. Austin, R. Cammi, C. Pomelli, J. W. Ochterski, P. Y. Ayala, K. Morokuma, G. A. Voth, P. Salvador, J. J. Dannenberg, V. G. Zakrzewski, S. Dapprich, A. D. Daniels, M. C. Strain, O. Farkas, D. K. Malick, A. D. Rabuck, K. Raghavachari, J. B. Foresman, J. V. Ortiz, Q. Cui, A. G. Baboul, S. Clifford, J. Cioslowski, B. B. Stefanov, G. Liu, A. Liashenko, P. Piskorz, I. Komaromi, R. L. Martin, D. J. Fox, T. Keith, M. A. Al-Laham, C. Y. Peng, A. Nanayakkara, M. Challacombe, P. M. W. Gill, B. Johnson, W. Chen, M. W. Wong, C. Gonzalez, J. A. Pople, *Gaussian 03, Revision C.02*, Gaussian, Inc., Wallingford CT **2004**.
- [33] J. Tomasi, R. Cammi, *J. Comput. Chem.* **1995**, *16*, 1449.
- [34] W. C. Vosburgh, G. R. Copper, *J. Am. Chem. Soc.* **1941**, *63*, 437.
- [35] S. Saureu, C. de Graaf, *Phys. Chem. Chem. Phys.* **2016**, *18*, 1233.
- [36] J. Q. Umberger, V. K. LaMer, *J. Am. Chem. Soc.* **1945**, *67*, 1099.
- [37] C. Preti, G. Tosi, M. Massacesi, G. Ponticelli, *Spectrochim. Acta* **1976**, *32*, 1779.
- [38] N. Tezer, N. Karakus, *J. Mol. Model.* **2009**, *15*, 223.
- [39] M. Pordel, S. Ramezani, M. Jajarmi, M. Sokhanvar, *Russ. J. Bioorg. Chem.* **2016**, *42*, 106.

- [40] M. Pordel, A. Abdollahi, B. Razavi, *Russ. J. Bioorg. Chem.* **2013**, 39, 240.
- [41] B. Tweedy, *Phytopathology* **1964**, 55, 910.

SUPPORTING INFORMATION

Additional Supporting Information may be found online in the supporting information tab for this article.

How to cite this article: Ramezani S, Pordel M, Davoodnia A. Synthesis, spectral, DFT calculations and antibacterial studies of Fe(III) complexes of new fluorescent Schiff bases derived from imidazo[4',5':3,4]benzo[1,2-c]isoxazole. *Appl Organometal Chem.* 2017;e4178. <https://doi.org/10.1002/aoc.4178>